A New Polytopic Bis-diazacrown-ether-polypyridine Ligand and Its Complexes with Zn(II) Salts and Mononuclear and Dendritic Ru(II) Precursors. Synthesis, Absorption Spectra, Redox Behavior, and Luminescence Properties

Frédérique Loiseau,[†] Cinzia Di Pietro,[†] Scolastica Serroni,[†] Sebastiano Campagna,*[,†] Antonino Licciardello,[‡] Amedea Manfredi,[§] Gianluca Pozzi,[§] and Silvio Quici*[,§]

Dipartimento di Chimica Inorganica, Chimica Analitica e Chimica Fisica, Università di Messina, via Sperone 31, I-98166 Messina, Italy, Dipartimento di Scienze Chimiche, Università di Catania, Viale Andrea Doria, I-95100 Catania, Italy, and Centro CNR and Dipartimento di Chimica Organica e Industriale, Università di Milano, I-20133 Milano, Italy

Received March 27, 2001

The new polytopic receptor **1** containing two terpyridine, one phenanthroline, and two diazacrown-ether sites has been prepared using a modular approach. Such a new species contains several pieces of information in its structure which can be processed by different metal ions to give different supramolecular inorganic architectures. Actually, reaction of **1** with $Zn(CH_3COO)_2$ in methanol, and subsequent anion exchange, afforded the intramolecular ring-type $[Zn(\mathbf{1})]^{2+}$ complex, which appears to be formed by a self-assembling reaction. A different synthetic approach, stepwise synthesis, allowed us to synthesize the two multicomponent compounds $[(bpy)_2Ru(\mu\text{-}\mathbf{1})Ru(bpy)_2]^{4+}$ (**Ru2**; bpy = 2,2′-bipyridine) and $[\{(bpy)_2Ru(\mu\text{-}2,3\text{-}dpp)\}_2Ru(\mu\text{-}\mathbf{1})Ru\{(\mu\text{-}2,3\text{-}dpp)Ru(bpy)_2\}_2]^{12+}$ (**Ru6**; 2,3-dpp = 2,3-bis(2-pyridyl)pyrazine). The absorption spectra and luminescence properties of **1** and $[Zn(\mathbf{1})]^{2+}$ are dominated by $\pi \rightarrow \pi^*$ transitions and excited states. The absorption spectra of the ruthenium compounds are dominated by ligand-centered (LC) bands in the UV region and metal-to-ligand charge-transfer (MLCT) bands in the visible. The latter compounds undergo several reversible metal-centered oxidations and ligand-centered reductions in the potential window investigated (−2.0/+2.0 V versus SCE) and exhibit MLCT luminescence in both acetonitrile fluid solution at room temperature and in butyronitrile rigid matrix at 77 K. Both the redox and photophysical properties of **Ru2** and **Ru6** can be assigned to specific subunits of the multicomponent structures. The data indicate that the $\{Ru(bpy)_2\}^{2+}$ and the dendritic $\{Ru[(\mu\text{-}2,3\text{-}dpp)Ru(bpy)_2]_2\}^{6+}$ fragments appended to the polytopic **1** ligands behave as independent components of the multicomponent arrays.

Luminescent and redox-active multicomponent species are the focus of intense studies because they play key roles in the development of supramolecular systems capable of performing photochemical light energy conversion[1] and for the elaboration of information at the molecular level.[2] Many different molecular arrangements are explored, ranging from dendrimers,[3] molecular wires,[4] racks, ladders and grids,[5] molecular squares,[6] variously interlocked systems, such as catenanes and rotaxanes,[2d,7] and so on.

It is indeed clear that on increasing the variety of the available somewhat sophisticated structures, the possibilities offered to the chemists ingenuity in tackling specific problems will also

* To whom correspondence should be addressed.
[†] Università di Messina.
[‡] Università di Catania.
[§] Università di Milano.

(1) The literature on this topic is too large to be exhaustively quoted. For some recent, representative books and review articles, see: (a) Balzani, V.; Scandola, F. *Supramolecular Chemistry*; Horwood: Chichester, U.K., 1991. (b) Gust, D.; Moore, T. A.; Moore, A. L. *Acc. Chem. Res.* **1993**, *26*, 198. (c) Hagfelt, A.; Graetzel, M. *Chem. Rev.*, **1995**, *95*, 49. (d) Balzani, V.; Juris, A.; Venturi, M.; Campagna, S.; Serroni, S. *Chem. Rev.* **1996**, *96*, 759. (e) Harriman, A.; Ziessel, R. *Chem. Commun.* **1996**, 1707. (f) Collin, J.-P.; Gaviña, P.; Sauvage, J.-P. *New J. Chem.* **1997**, *21*, 525. (g) Bignozzi, C. A.; Schoonover, J. R.; Scandola, F. *Prog. Inorg. Chem.* **1997**, *44*, 1. (h) De Cola, L.; Belser, P. *Coord. Chem. Rev.* **1998**, *177*, 301. (i) Collin, J.-P.; Gaviña, P.; Heitz, V.; Sauvage, J.-P. *Eur. J. Inorg. Chem.* **1998**, 1. (j) Choppinet, P.; Jullien, L.; Valeur, B. *Chem. Eur. J.* **1999**, *5*, 3666. (k) Barigelletti, F.; Flamigni, L. *Chem. Soc. Rev.* **2000**, *29*, 1. (l) Hu, Y.-Z.; Tsukiji, S.; Shinkai, S.; Oishi, S.; Hamachi, I. *J. Am. Chem. Soc.* **2000**, *122*, 241. (m) Hissler, M.; Connick, W. B.; Geiger, D. K.; McGarrah, J. E.; Lipa, D.; Lachicotte, R. J.; Eisenberg, R. *Inorg. Chem.* **2000**, *39*, 447. (n) Hissler, M.; McGarrah, J. E.; Connick, W. B.; Geiger, D. K.; Cummings, S. D.; Eisenberg, R. *Coord. Chem. Rev.* **2000**, *208*, 115.

(2) (a) Balzani, V.; Credi, A.; Scandola, F. In *Transition Metals in Supramolecular Chemistry*; Fabbrizzi L, Poggi, A., Eds; Kluwer: Dordrecht, The Netherlands, 1994; p 1. (b) Gilat, S. L.; Kawai, S. H.; Lehn, J.-M. *Chem. Eur. J.* **1995**, *1*, 275. (c) De Silva, A. P.; McClenaghan, N. D. *J. Am. Chem. Soc.* **2000**, *122*, 3965. (d) Balzani, V.; Credi, A.; Raymo, F.; Stoddart, J. F. *Angew. Chem., Int. Ed.* **2000**, *39*, 3348. (e) Jiménez, M. C.; Dietrich-Buckerer, C.; Sauvage, J.-P. *Angew. Chem., Int. Ed.* **2000**, *39*, 3285.

(3) (a) Campagna, S.; Denti, G.; Serroni, S.; Juris, A.; Venturi, M.; Ricevuto, V.; Balzani, V. *Chem. Eur. J.* **1995**, *1*, 211. (b) Newkome, G. R.; Cardullo, F.; Constable, E. C.; Moorefield, C. N.; Cargill Thompson, A. M. W. *J. Chem. Soc., Chem. Commun.* **1993**, 925. (c) Devadoss, C.; Bharathi, P.; Moore, J. S. *J. Am. Chem. Soc.* **1996**, *118*, 9635. (d) Jiang, D.-L.; Aida, T. *J. Am. Chem. Soc.* **1998**, *120*, 10895. (e) Archut, A.; Azzellini, G. C.; Balzani, V.; De Cola, L.; Vögtle, F. *J. Am. Chem. Soc.* **1998**, *120*, 12187. (f) Gilat, S. L.; Adronov, A.; Fréchet, J. M. J. *Angew. Chem., Int. Ed.* **1999**, *38*, 1422. (g) Balzani, V.; Ceroni, P.; Gestermann, S.; Kauffmann, C.; Gorka, M.; Vögtle, F. *Chem. Commun.* **2000**, 855. (h) Tsuda, K.; Dol, G. C.; Gensch, T.; Hofkens, J.; Latterini, L.; Weener, J. W.; Meijer, E. W.; De Schryver, F. C. *J. Am. Chem. Soc.* **2000**, *122*, 3445.

(4) (a) Barigelletti, F.; Flamigni, L.; Collin, J.-P.; Sauvage, J.-P. *Chem. Commun.* **1997**, 333. (b) Davies, W. B.; Svec, W. A.; Ratner, M. A.; Wasielewski, M. R. *Nature* **1998**, *369*, 60.

10.1021/ic010338+ CCC: $20.00
Published on Web 12/01/2001

increase. This is, for example, the case for the design of artificial light-harvesting systems; many efficient artificial antennas have been recently obtained, which differ significantly in molecular shapes and synthetic approaches, although the basic design principles (to build up multichromophoric systems in a structurally organized and functionally integrated fashion) remain the same.[8]

For the preparation of elaborated, made-to-order multicomponent systems the design of suitable polytopic receptors (or, more appropriately, polytopic ligands, if we deal with metal-containing architectures) is of large importance. Such polytopic receptors/ligands can be designed to contain in their structures codes which can be processed by suitable metal ions (which in their turn carry specific interactional algorithms) to produce specific supramolecular inorganic architectures.[9] The specific interactional algorithms include, among other factors, not only the preferred geometrical arrangements of the ligands around the metal ions (octahedral, tetrahedral, etc.) but also the metal−ligand bond strength, which ultimately makes the final architecture be determined by thermodynamics or kinetics.

Here we report: i) the synthesis of the new polytopic ligand **1** (Figure 1), which contains three different coordination domains (phenanthroline, terpyridine, and diazacrown-ether subunits) and, depending on the metal ion and the procedure followed in the complexation process, can afford complexes with different nuclearities and architectures; ii) the complexation behavior of **1**, which allowed the preparation of the ring-type $[Zn(\mathbf{1})]^{2+}$, the dinuclear $[(bpy)_2Ru(\mu\text{-}\mathbf{1})Ru(bpy)_2]^{4+}$ (**Ru2**; bpy = 2,2′-bipyridine), and the hexanuclear $[\{(bpy)_2Ru(\mu\text{-}2,3\text{-}dpp)\}_2Ru(\mu\text{-}\mathbf{1})Ru\{(\mu\text{-}2,3\text{-}dpp)Ru(bpy)_2\}_2]^{12+}$ (**Ru6**; 2,3-dpp = 2,3-bis(2′-pyridyl)-pyrazine) ruthenium (II) complexes; and iii) the study of the absorption spectra, luminescence properties, and redox behavior of all the new compounds.

Figure 1 shows the structural formulas of **1** and $[Zn(\mathbf{1})]^{2+}$, whereas Figure 2 reports the structural formulas of **Ru2** and **Ru6**. The two trinuclear moieties $\{Ru[(\mu\text{-}2,3\text{-}dpp)Ru(bpy)_2]_2\}^{6+}$ connected to **1** in complex **Ru6** are trinuclear first generation dendrons belonging to a large series of luminescent and redox-active metal-based dendrimers;[3a,10] therefore, complex **Ru6** can be viewed as the first example of metal-based dendritic branches connected by multiazacrown ether receptors.

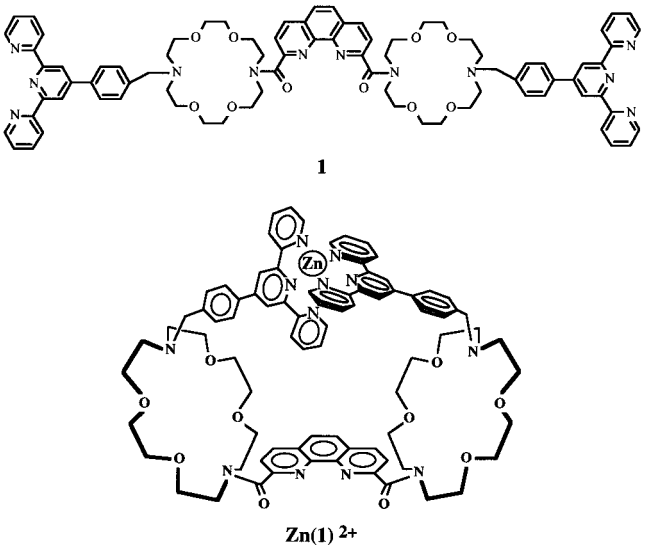

Figure 1. Structural formulas of **1** and of $[Zn(\mathbf{1})]^{2+}$.

It can also be noted that $[Zn(\mathbf{1})]^{2+}$ represents an example of self-assembly, while the ruthenium complexes have been prepared by employment of the stepwise synthetic procedure. The two different synthetic approaches are a consequence of the different chemistries of zinc and ruthenium ions, which apply different interaction algorithms in decoding the information embedded in **1**, on the basis of the various stabilities of the corresponding metal-polypyridine assemblies. The investigation reported here makes in evidence the different behavior of the same coordination domains (i.e., the terpyridine ones) toward the two substrates.

Results

Condensation of 4-benzyl-1,7,10,16-tetraoxa-4,13-diazacyclooctadecane, **2**,[11] with 1,10-phenanthroline-2,9-bis-carboxylic acid chloride, **3**,[12] carried out in dry CH_2Cl_2 and in the presence of diazabicyclooctane (DABCO) as base, afforded **4** in 49% yield after column chromatography. Debenzylation of **4** was achieved by catalytic hydrogenation at room temperature and $P = 1$ atm, in acetic acid, and using Pd/C-5% as catalyst. The bis-diaza derivative **5** obtained in 90% yield was then alkylated with 4′-(1-phenyl-*p*-bromomethyl)-2,2′:6′,2″-terpyridine, **6**,[13] in refluxing acetonitrile and in the presence of solid Na_2CO_3 as base to give **1** in 95% yield. The synthetic procedure is reported in Scheme 1.

The presence of various coordination domains in the structure of **1** makes this species quite versatile for the coordination of several substrates. In particular, the high flexibility of **1**

(5) (a) Baxter, P. N. W.; Lehn, J.-M.; Fisher, J.; Youinou, M. T. *Angew. Chem., Int. Ed. Engl.* **1994**, *33*, 2284. (b) Hanan, G. S.; Arana, C. R.; Lehn, J.-M.; Baum, G.; Fenske, D. *Chem. Eur. J.* **1996**, *2*, 1292. (c) (a) Credi, A.; Balzani, V.; Campagna, S.; Hanan, G. S.; Arana, C. R.; Lehn, J.-M. *Chem. Phys. Lett.* **1995**, *243*, 105. (d) Hasenknopf, B.; Hall, J.; Lehn, J.-M.; Balzani, V.; Credi, A.; Campagna, S. *New J. Chem.* **1996**, *20*, 725. (e) Ceroni, P.; Credi, A.; Balzani, V.; Campagna, S.; Hanan, G. S.; Arana, C. R.; Lehn, J.-M. *Eur. J. Inorg. Chem.* **1999**, 1409.

(6) (a) Drain, C. M.; Lehn, J.-M. *J. Chem. Soc., Chem. Commun.* **1994**, 2313. (b) Olenyuk, B.; Fechtenkotter, A.; Stang, P. J. *J. Chem. Soc., Dalton Trans.* **1998**, 1707. (c) Fujita, M. *Chem. Soc. Rev.* **1998**, 417. (d) Lo Schiavo, S.; Pocsfalvi, G.; Serroni, S.; Cardiano, P.; Piraino, P. *Eur. J. Inorg. Chem.* **2000**, 1371.

(7) (a) Armaroli, N.; De Cola, L.; Balzani, V.; Sauvage, J.-P.; Dietrich-Buchecker, C. O.; Kern, J.-M.; Bailal, A. *J. Chem. Soc., Dalton Trans.* **1993**, 3241. (b) Amabilino, D. B.; Stoddart, J. F. *Chem. Rev.* **1995**, *95*, 2725. (c) Armaroli, N.; Diederich, F.; Dietrich-Buchecker, C. O.; Flamigni, L., Marconi, G.; Nierengarten, J.-F.; Sauvage, J.-P. *Chem. Eur. J.* **1998**, *4*, 406. (d) Flamigni, L.; Armaroli, N.; Barigelletti, F.; Chambron, J.-C.; Sauvage, J.-P.; Solladié, N. *New J. Chem.* **1999**, 1151.(e) Nielsen, M. B.; Lomholt, C.; Becher, J. *Chem. Soc. Rev.* **2000**, *29*, 153. (f) Fustin, C.-A.; Leigh, D. A.; Rudolph, P.; Timpel, D.; Zerbetto, F. *Chem. Phys. Chem.* **2000**, *1*, 97.

(8) Campagna, S.; Serroni, S.; Puntoriero, F.; Di Pietro, C.; Ricevuto, V. In *Electron Transfer in Chemistry*; Balzani, V., Ed.; VCH−Wiley: Weinheim, 2001; Vol. 5, p 186.

(9) (a) Lehn, J.-M. *Chem. Eur. J.* **2000**, *6*, 2097. (b) Funeriu, D. P.; Lehn, J.-M.; Fromm, K. M.; Fenske, D. *Chem. Eur. J.* **2000**, *6*, 2103.

(10) (a) Denti, G.; Campagna, S.; Serroni, S.; Ciano, M.; Balzani, V. *J. Am. Chem. Soc.* **1992**, *114*, 2944. (b) Serroni, S.; Denti, G.; Campagna, S.; Juris, A.; Ciano, M.; Balzani, V. *Angew. Chem., Int. Ed. Engl.* **1992**, *31*, 1493. (c) Juris, A.; Balzani, V.; Campagna, S.; Denti, G.; Serroni, S.; Frei, G.; Güdel, H. U. *Inorg. Chem.* **1994**, *33*, 1491. (d) Serroni, S.; Juris, A.; Campagna, S.; Venturi, M.; Denti, G.; Balzani, V. *J. Am. Chem. Soc.* **1994**, *116*, 9086. (e) Serroni, S.; Juris, A.; Venturi, M.; Campagna, S.; Resino Resino, I.; Denti, G.; Credi A.; Balzani, V. *J. Mater. Chem.* **1997**, *7*, 1227. (f) Balzani, V.; Campagna, S.; Denti, G.; Juris, A.; Serroni, S.; Venturi, M. *Acc. Chem. Res.* **1998**, *31*, 26. (g) Ceroni, P.; Paolucci, F.; Paradisi, C.; Juris, A.; Roffia, S.; Serroni, S.; Campagna, S.; Bard, A. J. *J. Am. Chem. Soc.* **1998**, *120*, 5480. (h) Venturi, M.; Serroni, S.; Juris, A.; Campagna, S.; Balzani, V. *Top. Curr. Chem.* **1998**, *197*, 193.

(11) Quici, S.; Manfredi, A.; Pozzi, G.; Cavazzini, M.; Rozzoni, A. *Tetrahedron* **1999**, *55*, 10487.

(12) Chandler, C. J.; Deady L. W.; Reiss, J. A. *J. Heterocyc. Chem.* **1981**, *18*, 599.

(13) Constable, E. C.; Smith, D. R. *Supramol. Chem.* **1994**, *4*, 5.

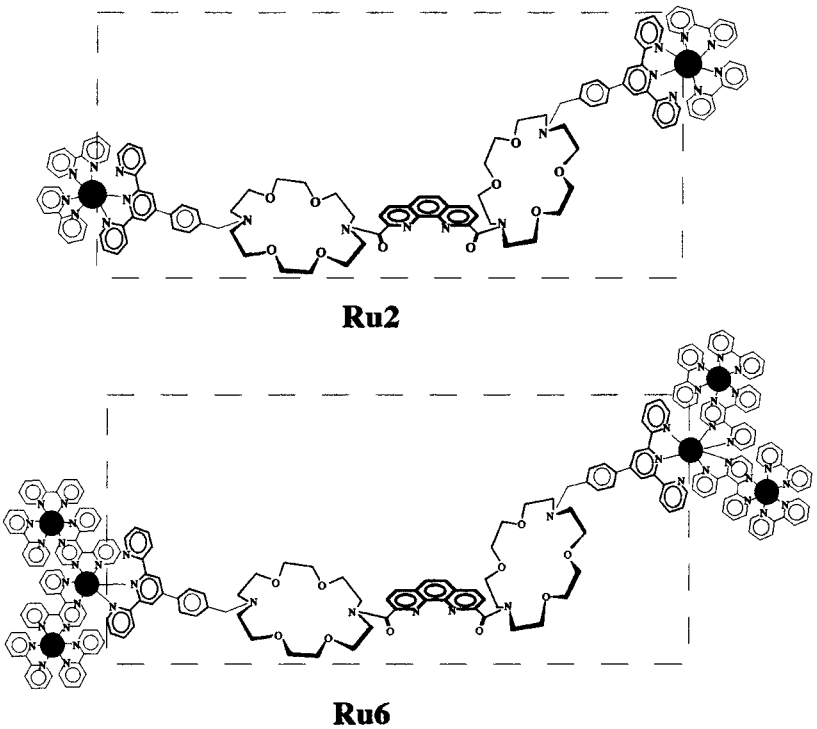

Figure 2. Structural formulas of complexes **Ru2** and **Ru6**. Ligand **1** is framed. Solid circles stand for ruthenium metals.

Scheme 1. Synthesis of the Multitopic Ligand **1**

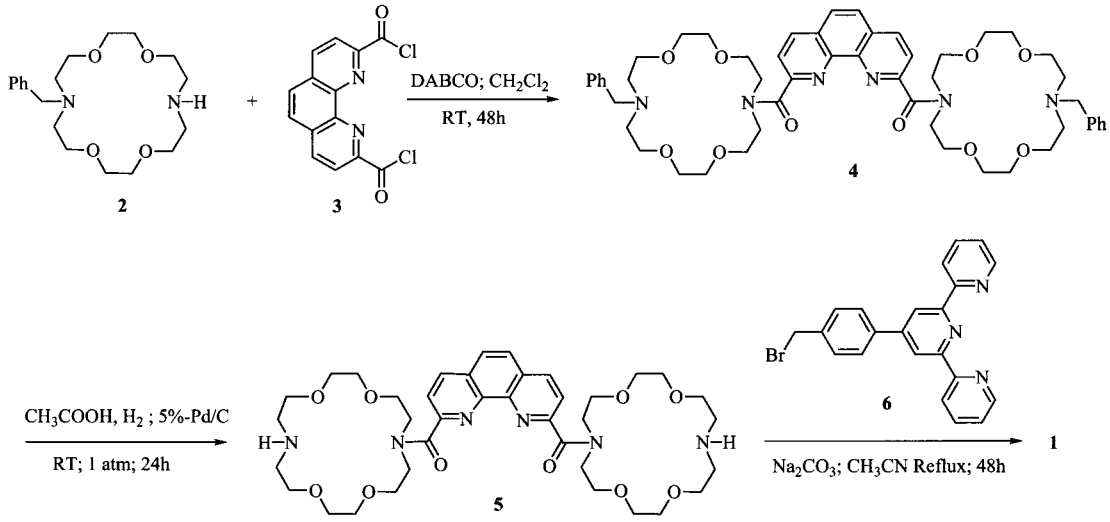

prompted us to explore the possibility of forming a molecular ring upon metal complexation. Because of the known ability of 2,2′,2″-terpyridine (terpy) ligands to coordinate Zn(II) cation,[14,15] the preparation of such a molecular ring was attempted by reacting **1** and $Zn(CH_3COO)_2$, in 1:1 molar ratio, in methanol solution under reflux. After anion exchange with NH_4PF_6, a new compound was obtained in 78% yield, which was identified as the intramolecular $[Zn(\mathbf{1})](PF_6)_2$ complex (see Figure 1) on the basis of the following. (i) A comparison between the ^{1}H NMR spectra in CD_3CN of the free ligand and of the Zn(II) compound showed that the relevant terpyridine protons shifted from 8.65 to 8.95 ppm upon complexation, which is in agreement with the involvement of both the terpy sites of **1** in metal binding.[16] (ii) Elemental analysis excluded the dimeric nature of the complex, i.e., $[(\mathbf{1})Zn(\mathbf{1})]^{2+}$, and was consistent with a ligand:Zn^{2+} 1:1 ratio. (iii) Time-of-flight secondary ions mass spectroscopy (TOF−SIMS) data confirm the proposed structure. Indeed, (Figure 3) in the high mass region of the spectrum, some peaks correspond to the emission of (quasi)-molecular fragments. In particular, the peak around *m*/*z* 1464 corresponds to the cationic complex [Zn(**1**)] with the probable loss of a proton. The peak at *m*/*z* 1483 corresponds to the cationic complex [Zn(**1**)] with an additional fluoride ion

(14) Ohno, T.; Kato, S. *Bull. Chem. Soc. Jpn.* 1**974**, *47*, 2953.
(15) Albano, G.; Balzani, V.; Constable, E. C.; Maestri, M.; Smith, D. R. *Inorg. Chim. Acta* **1998**, *277*, 225.

(16) The aromatic region of the ^{1}H NMR spectrum of the free ligand in CD_3CN is more complicated with respect to the corresponding one in $CDCl_3$ (described in the experimental) and can be referred substantially as three unresolved multiplets, namely: δ 7.35−7.47 (m, 8H, H,^{5}H$^{5''}$ −terpy, H^3, H^5 −C_6H_4); 7.55−8.03 (m, 12H, H^3, H$''$ −terpy, H,^{5}H,^{6} H,^{4} H^7 −phen, H^2, H^6 −C_6H_4); 8.55−8.75 (m, 14H, H^3, H,^{6}H$^{3'}$, H$^{5'}$, H$^{3''}$, H$^{6''}$ −terpy, H^3, H^8 −phen). The ^{1}H NMR spectrum of the aromatic region of the zinc complex in CD_3CN is δ 7.25−7.45 (m, 4H, H^3, H^5 −C_6H_4); 7.50−8.62 (m, 22H); 8.65−8.78 (m, 4H, H$^{3'}$, H$^{5'}$ −terpy); 8.90−9.07 (m, 4H, H,^{6}H$^{6'}$ −terpy).

Table 1. Spectroscopic and Photophysical Data for the Absorption of the New Compounds, the Maxima of the Spin-Allowed LC and MLCT Bands Are Given

compound	absorption[a] λ_{max}/nm (ϵ/$M^{-1}cm^{-1}$)	Luminescence, 298 K[a]			77 K	
		λ_{max}/nm	τ/ns	Φ	λ_{max}/nm	τ/μs
1	279 (110000)	351	2	5×10^{-3}		
$Zn(\mathbf{1})^{2+}$	284 (69200)	366	6	8×10^{-3}		
	320 (27000)					
$[Ru(bpy)_3]^{2+}$	452 (13000)	610	170	0.01	582[b]	5.1[b]
$[(bpy)Ru\{(\mu\text{-}2,3\text{-}dpp)Ru(bpy)_2\}_2]^{6+}$ [c]	282 (193400)	804	75	1×10^{-3}	721[d]	1.8[d]
	425 (35700)					
	545 (23500)					
Ru2	235 (80400)	631	8	4×10^{-3}	611[e]	1.4[e]
	286 (143200)					
	453 (26800)					
Ru6	239 (144600)	791	94	9×10^{-4}	710[e]	2.4[e]
	279 (229300)					
	422 (43400)					
	532 (65200)					

[a] In air-equilibrated CH_3CN solution. [b] In butyronitrile/propionitrile (5:4 v/v) rigid matrix. [c] From ref 10a. [d] In MeOH/EtOH (4:1 v/v) rigid matrix. [e] In butyronitrile rigid matrix.

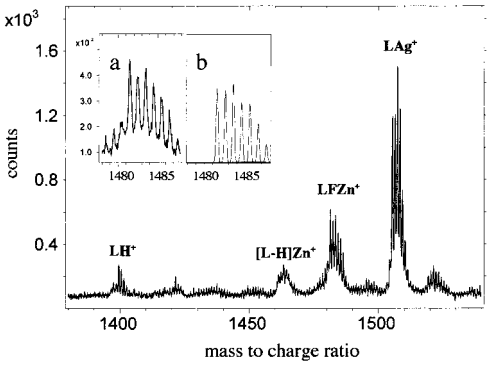

Figure 3. High mass region of the TOF−SIMS spectrum of $[Zn(\mathbf{1})](PF_6)_2$. The symbol **L** in the peak labels stays for structure **1**. The inset shows the experimental (a) and calculated (b) isotopic distribution of peak $LFZn^+$.

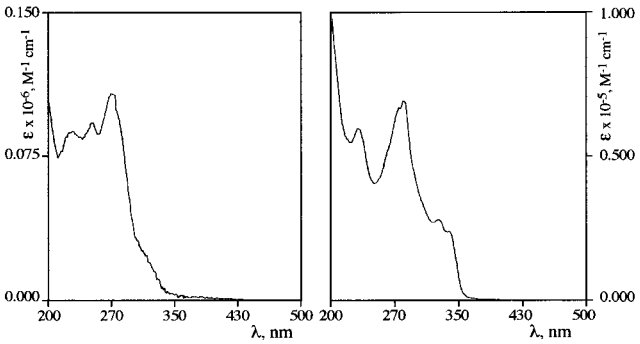

Figure 4. Absorption spectra in acetonitrile solution of **1** (left) and $[Zn(\mathbf{1})]^{2+}$ (right).

attached. The assignment is supported by the isotopic distribution (compare the experimental (a) and calculated (b) distributions in the inset of Figure 3) and by the exact mass (1481.53 observed versus 1481.59 calculated for the first peak of the distribution). It must be noted that fluorine attachment is not unexpected for such systems; indeed this has been observed[17] in other complexes containing PF_6^- counterions and is thought to originate from their fragmentation. As for the strong peak on the right-hand side of Figure 3, it is assigned to an $[Ag(\mathbf{1})]^+$ structure, due to the exchange of the metal with silver substrate during the measurement. A complete interpretation of such exchange is beyond the aim of this paper and will not be discussed further.

Moreover, reactions carried out with different molar ratios of **1** and $Zn(CH_3COO)_2$, namely 1:2, 2:1, or 4:1, univocally yielded the same compound described above, and the reactants in excess could be isolated unchanged at the end of the reaction. These findings demonstrate that the molecular ring $[Zn(\mathbf{1})]^{2+}$ is stable compared to the polymeric compounds which could be formed by intermolecular complexation. It was also found that $[Zn(\mathbf{1})]^{2+}$ may be generated in situ from an acetonitrile solution of **1** by adding an excess of solid $Zn(CH_3COO)_2$.

Reaction of **1** with the "complex−metal"[10] precursors $Ru(bpy)_2Cl_2$ and $[Cl_2Ru\{(\mu\text{-}2,3\text{-}dpp)Ru(bpy)_2\}_2]^{4+}$ under reflux conditions, followed by counterion exchange with excess NH_4PF_6 at room temperature, led to the formation of two new complexes in high yields, the dinuclear complex **Ru2** and the hexanuclear complex **Ru6**, respectively (see Figure 2). After substitution of the labile chloro ligands, the terpyridine subunits bind the metal centers utilizing two nitrogen atoms. The phenanthroline site does not compete with the terpyridine ones because the former is much more hindered.

The different reactivities of zinc and ruthenium precursors with **1** are assigned to the different stabilities of the metal−polypyridine assemblies. The zinc−terpyridine is a rather weak assembly, so the system can explore several possibilities and evolve toward thermodynamic minima. In the present case, the ring-type $[Zn(\mathbf{1})]^{2+}$ species evidently identifies a significant thermodynamic minimum for the system, and the synthesis of this species is a typical case of self-assembly. On the contrary, the linkage between ruthenium(II) and terpyridine is quite stable,[18] so the final product is governed by kinetics and, when several possibilities are exploitable, highly polydisperse polymeric systems are obtained. This reason made it necessary to employ the stepwise synthetic approach in the synthesis of the ruthenium(II) species reported here.

The electronic absorption spectra in acetonitrile of the free ligand **1** (Table 1, Figure 4) exhibits an intense maximum at $\lambda = 279$ nm (ϵ around 10^6 M^{-1} cm^{-1}) followed by a less intense maximum at about $\lambda = 260$ nm. The absorption spectrum of $[Zn(\mathbf{1})]^{2+}$ (Figure 4, Table 1**)** shows a structured band at around $\lambda = 320$ nm and the peak maximum at $\lambda = 284$ nm (ϵ in the range 10^5-10^6 M^{-1} cm^{-1}). The absorption spectra of both the

(17) Denti, G.; Serroni, S.; Sindona, G.; Uccella, N. *J. Am. Soc. Mass Spetrom.* **1993**, *4*, 306.
(18) (a) Juris, A.; Balzani, V.; Barigelletti, F.; Campagna, S.; Belser, P.; von Zelewsky, A. *Coord. Chem. Rev.* **1988**, *84*, 85. (b) De Armond, M. K.; Carlin, C. M. *Coord. Chem. Rev.* **1981**, *36*, 325.

Table 2. Half-Wave Potentials in Argon-Purged Acetonitrile Solution, 298 K, the Number of Exchanged Electrons Is Reported in Brackets

compound	$E_{1/2}$(ox) (V vs SCE)	$E_{1/2}$(red) (V vs SCE)
$[Zn(\mathbf{1})]^{2+}$	–	−1.31[a]
$[Ru(bpy)_3]^{2+}$[b]	+1.26 [1]	−1.35 [1]; −1.54 [1]; −1.79 [1]
$[(bpy)Ru\{(\mu\text{-}2,3\text{-}dpp)Ru(bpy)_2\}_2]^{6+}$[c]	+1.51 [2]; +1.95 [1]	−0.52 [1]; −0.66 [1]; −1.13 [1];−1.23 [1]; −1.47 [2]; −1.75 [2]
Ru2	+1.27 [2]	−1.29 [2]; −1.52 [2]; −1.84 [ads]
Ru6	+1.52 [4]; +2.00	−0.57 [2]; −0.68 [2]; −1.09 [2];−1.16 [2]; −1.43; −1.63[d]

[a] Irreversible process. This figure refers to the peak potential. [b] From ref 17a. [c] From ref 10a. [d] Overlapping waves are present at more negative potentials.

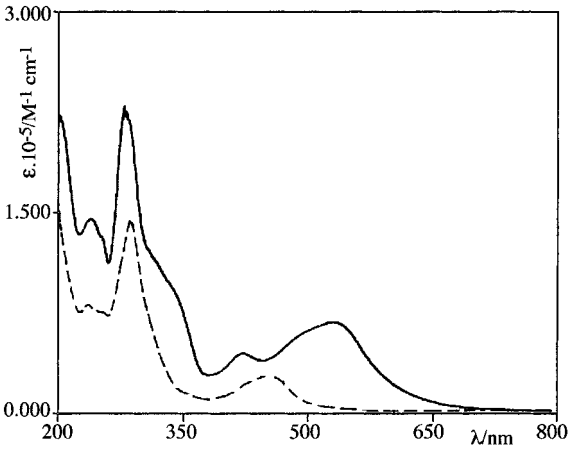

Figure 5. Absorption spectra of complexes **Ru2** (dashed line) and **Ru6** (solid line) in acetonitrile at room temperature.

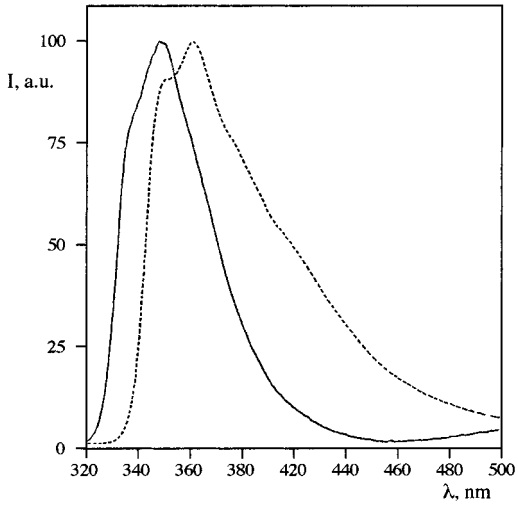

Figure 6. Luminescence spectra in acetonitrile solution of **1** (solid line) and $[Zn(\mathbf{1})]^{2+}$ (dashed line).

Ru complexes (Figure 5, Table 1) exhibit very intense bands in the UV region (ϵ in the range 80000−230000 M^{-1} cm^{-1}) and moderately intense bands in the visible region (ϵ in the range 25000−70000 M^{-1} cm^{-1}).

All the new compounds are luminescent; the emission spectrum of **1** (Figure 6 Table 1) exhibits a maximum at λ = 351 nm in acetonitrile at room temperature, it is not dependent on excitation wavelength (within the range 260−320 nm), and its decay is monoexponential and in the nanosecond time scale. The emission spectrum of $[Zn(\mathbf{1})]^{2+}$ (Figure 6, Table 1), while still occurring in the UV region, is significantly red-shifted with respect to the free ligand emission and is long lived. Furthermore, the emission quantum yield is enhanced with respect to that of the free ligand. Both the Ru compounds are luminescent at room temperature in acetonitrile fluid solution and at 77 K in butyronitrile rigid matrix. The uncorrected luminescence spectra are shown in Figure 7; the corrected emission maxima

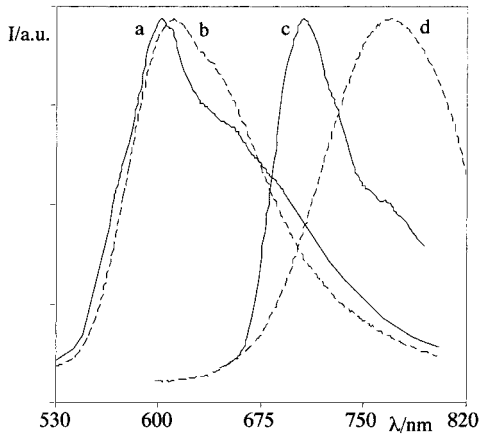

Figure 7. Luminescence spectra of complexes **Ru2** (77 K in butyronitrile, a; room temperature in acetonitrile, b) and **Ru6** (77 K in butyronitrile, c; room temperature in acetonitrile, d). The spectra shown are uncorrected for photomultiplier response. Corrected values for emission maxima are given in Table 1.

of the luminescence bands, the luminescence lifetimes, and the luminescence quantum yields are collected in Table 1. Luminescence decays are monoexponential and in the microsecond time scale at 77 K and two or three orders of magnitude lower at 298 K.

The ring-type zinc complex does not exhibit any oxidation process in the potential window examined (+2.00/−2.00 V versus SCE) in acetonitrile. On the contrary, an irreversible reduction process takes place at −1.31 V (peak value) followed by other irreversible ill-defined processes. The redox behavior of the free ligand, **1**, has not been investigated because of solubility problems. The cyclic and differential pulse voltammetry experiments of the ruthenium(II) complexes indicate that these species undergo several reversible oxidation and reduction processes in the potential window examined. The potential values are collected in Table 2. The oxidation and reduction processes of **Ru2** are bielectronic, as are the reduction processes of **Ru6**. This species undergoes two oxidation processes: the first one involves four electrons, while for the second one, it is impossible to determine the number of exchanged electrons because oxidation occurs too close to the potential limit. Indeed, its presence was only revealed by differential pulse voltammetry. For both complexes, wave overlapping and adsorption phenomena occur at most negative potentials. The cyclic voltammograms of complexes **Ru2** and **Ru6** are shown in Figures 8 and 9.

Discussion

Free Ligand 1 and the Ring-Type $[Zn(1)]^{2+}$ Complex. Absorption Spectra. On the basis of literature data, the peaks dominating the absorption spectrum of **1** (Figure 4) may be assigned to spin-allowed $\pi-\pi^*$ transitions centered in the polypyridine ligands.[18,19] In particular, the band at lower energy should receive contribution mainly from transitions involving

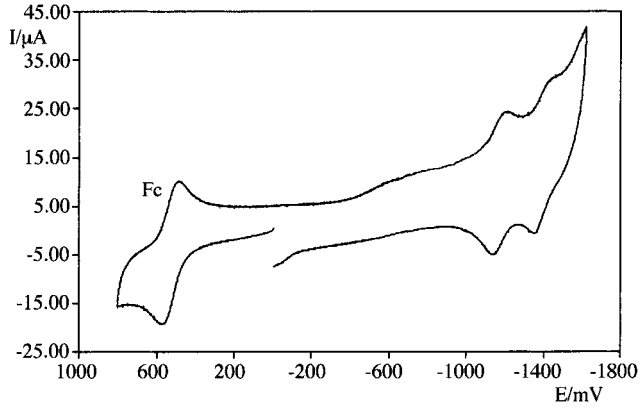

Figure 8. Cyclic voltammogram of complex **Ru2** in argon-purged acetonitrile solution. Only the reduction range is shown. Fc stands for ferrocene, used as internal standard. Sweep rate: 200 mV/sec.

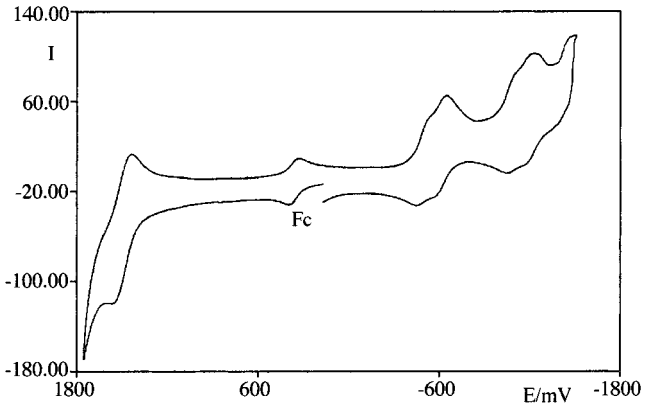

Figure 9. Cyclic voltammogram of complex **Ru6** in argon-purged acetonitrile solution. Sweep rate: 200 mV/sec.

the phenyl−terpyridine sites, and the band at higher energy receives contribution mainly from transitions involving the phenanthroline site. The low shoulder at about $\lambda = 320$ nm is assigned to n−π* transitions once more involving the polypyridine sites.[19]

The peaks dominating the absorption spectrum of $[Zn(\mathbf{1})]^{2+}$ (Figure 4) are also assigned to spin-allowed metal-perturbed $\pi-\pi$* transition involving the phenyl−terpyridine sites. It is indeed known that metal coordination shifts the polypyridine-based $\pi-\pi$* transitions to lower energies with respect to those occurring in the free ligand, and in the case of terpyridine ligands, a fine vibrational structure often appears at the lower-energy side of the main absorption band.[20]

Redox Behavior. The absence of oxidation processes for $Zn(\mathbf{1})^{2+}$ in the potential window examined was expected because metal oxidation is extremely difficult for the d^{10} Zn(II) species. The peak of the first irreversible reduction (Table 2) occurs at a potential typical for terpy-based reduction in metal complexes,[1d,18a] so we suggest that it is centered on the terpy ligand(s). The irreversibility of the process compared to the reversibility of terpy reduction in the ruthenium compounds (see later) is probably due to the lower stability of Zn(II)−polypyridine complexes compared to Ru(II)−polypyridine ones. Other reduction processes take place at more negative potentials, but they all are ill defined and will not be discussed further here.

Luminescence Properties. The emission of **1** (Figure 6) is assigned to phenylterpyridine-based fluorescence involving a $\pi-\pi$* level, based on the photophysical data of similar terpyridine-containing ligands.[19] Interestingly, the excitation spectrum, recorded at $\lambda = 380$ nm, fairly matches the absorption spectrum, therefore, indicating that efficient energy transfer occurs from the phenanthroline chromophore to the phenyl−terpyridine sites. Emission of $[Zn(\mathbf{1})]^{2+}$ is also assigned to fluorescence involving the phenylterpyridine-based $\pi-\pi$* levels, which are lowered in energy compared to the free ligand as a consequence of metal perturbation. It can be noted that the emission of $[Zn(\mathbf{1})]^{2+}$ is quite similar to that exhibited by $[Zn(terpy)_2]^{2+}$ under the same experimental conditions (terpy = 2,2′,2″-terpyridine), which was already assigned to metal-perturbed $\pi-\pi$* terpy-based fluorescence.[15] Interestingly, the emission of $[Zn(\mathbf{1})]^{2+}$ is slightly red-shifted compared to that of $[Zn(terpy)_2]^{2+}$ (emission maximum for this latter species is 353 nm,[15] while for $[Zn(\mathbf{1})]^{2+}$ it is 366 nm). This can be rationalized by considering that the presence of the phenyl substituent in the coordinating terpy subunits in **1** reduces the energy gap between π and π* orbitals of this latter species compared to terpy, thus lowering the $\pi-\pi$* level.

The enhanced rigidity of the molecular ring structure of $[Zn(\mathbf{1})]^{2+}$ compared to the free ligand is held responsible for the enhanced emission quantum yield and longer lifetime, most likely by slowing the nonradiative rate constants of the emitting levels because of restricted freedom degrees available for vibronically assisted excited-state radiationless decays.

Ruthenium(II) Complexes. Absorption Spectra. The very intense absorption bands in the region below 400 nm exhibited by **Ru2** and **Ru6** (Table 1, Figure 5) can be attributed to spin-allowed ligand-centered (LC) transitions. In particular, by comparison with literature data,[18a] the bands around 280 nm can mainly be assigned to bipyridine- and terpyridine-centered transitions, and the absorption feature around 320 nm, which is present in **Ru6** and absent in **Ru2**, can safely be assigned to 2,3-dpp-centered transitions, as already reported for other metal dendrimers containing such a bridging ligand.[10] The moderately intense absorption bands which dominate the visible region can be attributed to spin-allowed metal-to-ligand charge-transfer (MLCT) transitions. In particular, as far as complex **Ru6** is concerned, the band peaking at 422 nm is due to Ru → phenylterpy CT transitions, while the broad band peaking at 532 nm receives contributions from MLCT transitions involving the 2,3-dpp bridging ligands.

Redox Behavior. Complex **Ru6** exhibits a redox behavior comparable to that of the model trinuclear dendron $[(bpy)Ru\{(\mu\text{-}2,3\text{-}dpp)Ru(bpy)_2\}_2]^{6+}$ (Table 2, Figure 9).[21] A reversible tetraelectronic oxidation wave appears at +1.52 V followed by a less intense wave around +2.0 V, which is partly hidden by the limit of our potential window. Generally, oxidations of d^6 metal complexes containing polypyridine ligands are metal-centered and reversible. Because of its tetraelectronic nature and by comparison with the data of the trinuclear dendron,[21] the first oxidation wave can be attributed to four simultaneous and independent one-electron processes involving the peripheral metal centers. The second one is due to the oxidation of central metals, which are more difficult to oxidize than the peripheral centers because of the different electron donor abilities of the ligands.[10]

(19) Klessinger, M.; Michl, J. *Excited States and Photochemistry of Organic Molecules*; VCH: Weinheim, 1994.
(20) Guglielmo, G.; Ricevuto, V.; Giannetto, A.; Campagna, S. *Gazz. Chim. Ital.* **1989**, *119*, 457.
(21) (a) Denti, G.; Campagna, S.; Sabatino, L.; Serroni, S.; Ciano, M.; Balzani, V. *Inorg. Chem.* **1990**, *29*, 4750. (b) Puntoriero, F.; Serroni, S.; Licciardello, A.; Juris, A.; Venturi, M.; Ricevuto, V.; Campagna, S. *J. Chem. Soc., Dalton Trans.* **2001**, *7*, 1035−1042.

The reversible reduction waves of the hexanuclear compound can be assigned on the basis of the different electron densities of the ligands of the system. It is known that in polynuclear Ru(II) complexes containing 2,3-dpp as the bridging ligand and bpy as the peripheral ligands, each 2,3-dpp ligand is reduced twice before reduction of the peripheral ligands takes place.[10h] As a consequence, the first bielectronic reduction process of **2** is assigned to simultaneous first reduction of two 2,3-dpp bridges belonging to different dendron subunits. The second bielectronic reduction process can, therefore, be safely assigned to a simultaneous first reduction of the two remaining 2,3-dpp bridges. The third and fourth reduction processes, both bielectronic in nature, are assigned to the second reduction processes of the four bridging ligands, with the same sequence already discussed for the first two processes. Such an assignment is also supported by the difference between the first and third reduction potentials (≈500 mV), which is typical for the energy pairing in 2,3-dpp.[10] It is also interesting to note (Table 2) that the separation between the reduction processes corresponding to the first reductions (separation between first and second processes, 110 mV) is larger than the separation between the reduction processes corresponding to the second reduction (separation between third and fourth processes, 70 mV) of the bridge. This can be rationalized by considering that ligand−ligand interactions in metal complexes, inferred by the separation between the ligand-centered reduction potentials, are mainly mediated by the metal orbitals and depend on the energy gap between ligand and metal orbitals.[22] Upon first reduction, the ligand orbitals are raised in energy, so that such an energy gap increases and ligand−ligand interaction via metal orbitals decreases, leading to a reduced separation between the ligand-centered second reduction potentials.

At potentials more negative than −1.4 V, more intense, overlapping reduction waves appear, which are due to the two series of reductions involving the bipyridine and terpyridine ligands. Also, because of adsorption phenomena, those waves are difficult to assign unambiguously.

Complex **Ru2** shows a bielectronic reversible oxidation wave at +1.27 V, which can be assigned to the simultaneous and independent one-electron oxidation of the ruthenium centers. The first bielectronic reduction wave is assigned to the terpyridine moieties of the ligand, which are more easily reduced than the bipyridines due to the presence of the phenyl substituents. The first series of reversible reductions of the bipyridines appears at −1.52 V, and the second series appears at −1.84 V. At more negative potentials, the subsequent reduction waves of the bipyridine ligands are hidden by adsorption phenomena.

Luminescence Properties. In Ru(II) polypyridine complexes, emission usually originates from the lowest-lying triplet MLCT excited state.[18a,23] On the basis of the luminescence energies, lifetimes, and quantum yields given in Table 1, and the difference between the photophysical data at room temperature and at 77 K (Table 1, Figure 7), this designation also holds for the new compounds investigated here. In particular, emission of **Ru2** can be attributed, both at room temperature in fluid solution and at 77 K in rigid matrix, to a ^{3}MLCT state involving the phenylterpyridine ligands. In fact, the luminescence energy of **Ru2** is red-shifted with respect to $[Ru(bpy)_3]^{2+}$ (Table 1), in agreement with the redox data which indicate that the phenylterpyridine ligands are easier to reduce than the peripheral bipyridines (see above). It is interesting to note that the emission lifetime of **Ru2** is substantially shorter, at room temperature, than that of $[Ru(bpy)_3]^{2+}$ (Table 1). This may be due to the presence of the noncoordinating pyridine of the acceptor ligand. It is well-known indeed that bulky substituents in the six position of bpy ligands cause steric crowding around the octahedral metal center, decreasing the ligand field experienced by the metal and thus lowering the ^{3}MC level.[18a,23b] Because radiationless decay of the luminescent ^{3}MLCT state can be accelerated by thermal activation of upper-lying ^{3}MC states,[18a,23b] the lowering of such states leads to decreased quantum yields and shorter lifetimes. This effect cannot play any role at 77 K, however, the luminescence lifetime remains shorter compared to that of $[Ru(bpy)_3]^{2+}$, and the difference cannot be justified only on the basis of the energy gap law.[24] We have no simple explanation for such a result. We tentatively suggest that some moiety of the large ligand, **1**, could promote vibrational modes that lead to reduced excited-state lifetimes, also at 77 K.

As far as compound **Ru6** is concerned, the similarity between its emission properties and those of $[(bpy)Ru\{(\mu\text{-}2,3\text{-}dpp)Ru(bpy)_2\}_2]^{6+}$ (Table 1)[21] allows us to assign the emission of **Ru6** to the same subunit responsible for the emission of the trinuclear species, namely a ^{3}MLCT level involving the peripheral metals and the 2,3-dpp bridging ligands. Similar to what happened for the trinuclear compound $[(bpy)Ru\{(\mu\text{-}2,3\text{-}dpp)Ru(bpy)_2\}_2]^{6+}$, the constancy of the emission spectrum on changing excitation wavelength and the monoexponential decay indicate that the light absorbed by the $\{(terpy)Ru(2,3\text{-}dpp)_2\}^{2+}$ subunits is quantitatively transferred to the luminescent peripheral $\{(2,3\text{-}dpp)Ru(bpy)_2\}^{2+}$ chromophores of **Ru6**.

The complexes **Ru2** and **Ru6** bear additional receptor subunits. In particular, the azacrown subunits can accommodate alkaline and alkaline-earth cations as well as transition metal cations, such as Cu^{2+}.[25,26] A series of closely related terpy and bpy units attached to azacrowns has recently been published by Ward, Barigelletti, et al.[27] In those papers, it was reported that incorporation of an alkaline-earth cation within the azacrown moiety affected the photophysical properties of a dinuclear Re−Ru complex by inducing conformational changes and preventing the nitrogen atoms of the azacrown from acting as an electron-transfer quencher for the rhenium-based luminophore. However, most of these effects were related to the presence of the rhenium subunit. As far as the Ru-based emission is concerned, only a slight increase in luminescence lifetime at 77 K was obtained (proposed explanation was that the presence of cations within the azacrown cavity slows the nonradiative processes). In fact,

(22) Marcaccio, M.; Paolucci, F.; Paradisi, C.; Roffia, S.; Fontanesi, C.; Yellowlees, L. J.; Serroni, S.; Campagna, S.; Denti, G.; Balzani, V. *J. Am. Chem. Soc.* **1999**, *121*, 10081.

(23) (a) Crosby, G. A. *Acc. Chem. Res.* **1975**, *8*, 231. (b) Meyer, T. J. *Pure Appl. Chem.* **1986**, *58*, 1193.

(24) (a) Siebrand, W. *J. Chem. Phys.* **1967**, *46*, 440. (b) Caspar, J. V.; Meyer, T. J. *J. Phys. Chem.* **1983**, *87*, 952.

(25) See, for example: (a) *Chemosensors of Ion and Molecule Recognition*; Desvergne, J. P., Czarnick, A. W., Eds.; NATO ASI Series 492; Kluwer: Dordrecht, 1997. (b) Spichiger-Keller, U. E. *Chemical Sensors and Biosensors for Medical and Biological Applications*; Wiley−VCH: Weinheim, 1998. (c)de Silva, A. P.; Gunaratne, H. Q. N.; Gunnlaugsson, T.; Huxley, A. J. M.; McCoy, C. P.; Rademacher, J. T.; Rice, T. E. *Chem. Rev.* **1997**, *97*, 1515. (d) Di Pietro, C., Guglielmo, G.; Campagna, S.; Diotti, M.; Manfredi, A.; Quici, S. *New J. Chem.* **1998**, 1037. (e) Di Pietro, C.; Campagna, S.; Ricevuto, V.; Giannetto, M.; Manfredi, A.; Pozzi, G.; Quici, S. *Eur. J. Org. Chem.* **2001**, 587−594.

(26) Izatt, R. M.; Pawlak, K.; Bradshaw, J. S.; Bruening, R. L. *Chem. Rev.* **1991**, *91*, 1721.

(27) (a) Whittle, B.; Batten, S. R.; Jeffery, J. C.; Rees, L.; Ward, M. D. *J. Chem. Soc., Dalton Trans.* **1996**, 4249. (b) Bushell, K. L.; Couchman, S. M.; Jeffery, J. C.; Rees, L. H.; Ward, M. D. *J. Chem. Soc., Dalton Trans.* **1998**, 3397. (c) Encinas, S.; Bushell, K. L.; Couchman, S. M.; Jeffery, J. C.; Ward, M. D.; Flamigni, L.; Barigelletti, F. *J. Chem. Soc., Dalton Trans.* **2000**, 1783.

addition of K^+, Na^+, Ca^{2+}, and similar ions, including protons, does not modify the photophysical properties of the complexes **Ru2** and **Ru6** studied here. Indeed, in the Re−Ru dinuclear systems reported in the literature,[27] the azacrown and the Ru-based chromophores were connected by a simple methylene group, whereas in **Ru2** and **Ru6**, the azacrowns and chromophores are separated by a longer spacer. While large effects were not expected anyway, in the present compounds the longer spacer between the Ru chromophore(s) and the azacrowns probably makes the slight effects of the encapsulated cation on luminescence lifetime unsizable. On the contrary, Cu^{2+} was expected to quench **Ru2** luminescence by oxidative electron transfer (and maybe also by energy transfer).[28,29] However, even the addition of Cu^{2+} ions, which are expected to be strongly complexed by the azacrowns,[26] does not modify the photophysical properties of **Ru2**. We suggest that the inefficiency of the quenching process is due to the large distance between donor and acceptor partners coupled with the relatively short excited-state lifetime of the luminescent metal complex (Table 1).

Conclusions

The polytopic ligand, **1**, has been prepared through a flexible modular approach. Subsequent reaction of **1** with Zn^{2+} salts gives the supramolecular $[Zn(\mathbf{1})]^{2+}$ macrocycle. Reaction of the same ligand with $Ru(bpy)_2Cl_2$ and $[Cl_2Ru\{(\mu\text{-}2,3\text{-}dpp)Ru(bpy)_2\}_2]^{4+}$ under reflux conditions yields the dinuclear complex **Ru2** and the hexanuclear complex **Ru6**, respectively. In particular, compound **Ru6** is an example of a species containing dendritic branches decorating a multitopic receptor. While the synthesis of the zinc complex is an example of self-assembly, the preparation of the ruthenium compounds is based on a stepwise synthetic approach. The absorption spectra and photophysical properties of **1** and $[Zn(\mathbf{1})]^{2+}$ are dominated by $\pi \rightarrow \pi^*$ transitions and excited states, and the absorption and luminescence properties of the ruthenium compounds are dominated by MLCT transitions and excited states. Furthermore, the spectroscopic, photophysical, and redox properties of the new ruthenium compounds indicate that the metal and dendritic subunits connected to the terpyridine subunits of the multitopic ligand behave as independent components of the multicomponent arrays.

Experimental Section

Materials and Methods. The precursors $Ru(bpy)_2Cl_2$[30] and $[Cl_2Ru\{(\mu\text{-}2,3\text{-}dpp)Ru(bpy)_2\}_2](PF_6)_4$[31] were prepared as reported in the literature. Solvents were purified by using standard methods and dried if necessary. All commercially available reagents were used as received. However, the supporting electrolytes and the glassware employed for the electrochemical experiments were stored in an oven for at least 24 h before use. TLC was carried out on silica gel Si 60-F_{254}. Column chromatography was carried out on silica gel Si 60, mesh size 0.040−0.063 mm (Merck, Darmstadt, Germany). ^{1}H NMR (300 MHz) spectra were recorded with a Bruker AC 300 spectrometer. Elemental analysis were performed by the Departmental Service of Microanalysis (University of Milan). Melting points (uncorrected) were determined with a Buchi SMP-20 capillary melting point apparatus. TOF−SIMS measurements were performed in "static mode" (less than 5×10^{11} primary ions/cm^2) in a TOF−SIMS IV (ION-TOF) instrument using a pulsed gallium beam (25 keV, 1 pA, 0.8 ns pulse width). Samples were prepared as very thin layers by microsyringe deposition of an acetonitrile solution on etched silver, following literature procedures.[32] Electronic absorption spectra were recorded on a Kontron Uvikon spectrophotometer. Luminescence spectra were obtained with a Jobin Yvon-Spex Fluoromax-2. Emission lifetime measurements were carried out with a Edinburgh FL-900 time-correlated single-photon-counting (N_2 lamp, 337 nm; 3 ns lamp width), using a Marquadt algorithm to take into account the lamp contribution to the luminescence decay, when necessary. Luminescence quantum yields were obtained at room temperature (20°C) using the optically dilute method.[33] Anthracene in degassed ethanol solution was employed as the quantum yield standard ($\Phi = 0.27$)[34] for the free ligand and the zinc complexes, while $[Ru(bpy)_3]^{2+}$ (bpy = 2,2′-bipyridine) in aerated aqueous solution and $[Os(bpy)_3]^{2+}$ in deaerated acetonitrile solution were used as quantum yield standards for **Ru2** and **Ru6**, respectively, assuming values of 0.028[35] and 0.0066,[36] respectively. Electrochemical measurements were carried out in argon-purged acetonitrile at room temperature, with a PAR 273 multipurpose equipment interfaced to a PC. The working electrode was a glassy carbon (8 mm^2, Amel) electrode. The counter electrode was a Pt wire separated with a fine glass frit, and the reference electrode was a quasi-reference silver wire. Ferrocene was used as an internal standard. The concentration of the complexes was about 5×10^{-4} M. Tetrabutylammonium hexafluorophosphate was used as supporting electrolyte, and its concentration was 0.05 M. Cyclic voltammograms were obtained at scan rates of 20, 50, 200, and 500 mV/s. For reversible processes, half-wave potentials (versus SCE) were calculated as the average of the cathodic and anodic peaks. The criteria for reversibility were the separation between cathodic and anodic peaks, the close-to-unity ratio of the intensities of the cathodic and anodic currents, and the constancy of the peak potential on changing scan rate. The number of exchanged electrons was measured with differential pulse voltammetry (DPV) experiments performed with a scan rate of 20 mV/s, a pulse height of 75 mV, and a duration of 40 ms. For irreversible processes, the values reported are the peaks estimated by DPV.

Experimental uncertainties are as follows: absorption maxima, ± 2 nm; molar extinction coefficients, 10%; luminescence maxima, ± 5 nm; luminescence lifetimes, 10%; luminescence quantum yields, 20%; %; and redox potentials, ± 10 mV.

Synthesis. 2,9-Bis-(13-benzyl-1,7,10,16-tetraoxa-4,13-diazacyclooctadecane)-carbonyl-1,10-phenanthroline (4). A solution of 1,10-phenanthroline-2,9-bis-carboxylic acid chloride **3** (1.30 g, 3.44 mmol) in dry CH_2Cl_2 (30 mL) was slowly added at room temperature to a stirred solution of 4-benzyl-1,7,10,16-tetraoxa-4,13-diazacyclooctadecane **2** (2.42 g, 6.88 mmol) and DABCO (1.93 g, 17.20 mmol) in dry CH_2Cl_2 (80 mL), and the reaction mixture was stirred for 48 h. The reaction mixture was transferred into a separatory funnel, washed with H_2O (3×50 mL), and the organic phase evaporated under reduced pressure to afford 3.45 g of crude yellow viscous oil. Purification by column chromatography (silica gel, light petroleum/Et_2O 95/5) (silica gel, $CHCl_3/CH_3OH$ 9/1) gives **4** (1.58 g, yield = 49%) as a light yellow viscous oil. ^{1}H NMR ($CDCl_3$): δ 2.70−2.85 (m, 8H, CH_2N−Bn), 3.48 (s, 8H, CH_2O), 3.50−3.75 (m, 20H, CH_2O, PhCH_2N), 3.80−4.00 (m, 12H, CH_2O, CH_2NCO), 4.05−4.15 (m, 4H, CH_2NCO), 7.15−7.38 (m, 10H, C$_6H_5$), 7.85 (s, 2H, H,[5] H^6 −Phen), 8.00 (d, J = 9.4 Hz, 2H, H^4, H^7 −Phen), 8.30 (d, J = 9.4 Hz, 2H, H^3, H^8 −Phen). MS−FAB(+) m/z 960 [(M + Na^+], 937 [M]. Calcd for $C_{52}H_{68}N_6O_{10}$: 937. $C_{52}H_{68}N_6O_{10}$ Calcd: C, 66.64; H, 7.33; N, 8.96. Found: C, 66.30; H, 7.05; N, 8.80.

2,9-Bis-(1,7,10,16-tetraoxa-4,13-diazacyclooctadecane)-carbonyl-1,10-phenanthroline (5). A solution of **4** (1.58 g, 1.96 mmol) in CH_3-COOH (30 mL) was hydrogenated at room temperature and atmospheric

(28) (a) Roundhill, D. M. *Photochemistry and Photophysics of Metal Complexes*; Plenum: New York, 1994. (b) Fabbrizzi, L.; Poggi, A. *Chem. Soc. Rev.* **1995**, 197.

(29) The hexanuclear compound **Ru6** is a poor photoreductant, so electron-transfer quenching of **Ru6** luminescence by copper(II) is not expected to be efficient.

(30) Sullivan, B. P.; Salmon, D. J.; Meyer, T. J. *Inorg. Chem.* **1978**, *17*, 3334.

(31) (a) Campagna, S.; Denti, G.; Serroni, S.; Ciano, M.; Balzani, V. *Inorg. Chem.* **1991**, *30*, 3728. (b) Serroni, S.; Denti, G. *Inorg. Chem.* **1992**, *31*, 4251.

(32) Bletsos, I. V.; Hercules, D. M.; van Leyen, D.; Benninghoven, A. *Macromolecules* **1987**, *20*, 407.

(33) Demas, J. N.; Crosby, G. A. *J. Phys. Chem.* **1971**, *75*, 991.

(34) Dawson, W. R.; Windsor, M. W. *J. Phys. Chem.* **1968**, *72*, 3251.

(35) Nakamaru, K. *Bull. Chem. Soc. Jpn.* **1982**, *55*, 2697.

(36) Lumpkin, R. S.; Meyer, T. J. *J. Phys. Chem.* **1986**, *90*, 5307.

pressure in the presence of Pd/C, 5% (400 mg). The reaction mixture was filtered through a Celite plug, and the solvent was evaporated under reduced pressure. The residue was dissolved in CH_2Cl_2 (100 mL), washed with 10% aqueous Na_2CO_3, and the solvent evaporated to give **5** (1.15 g, yield = 90%) as a light yellow thick oil. ^{1}H NMR ($CDCl_3$): δ 2.65−2.80 (m, 10H, C*H*$_2$N*H*), 3.40 (s, 8H, C*H*$_2$O), 3.50−4.00 (m, 28H, C*H*$_2$O, C*H*$_2$NCO), 4.02−4.10 (m, 4H, C*H*$_2$NCO), 7.72 (s, 2H, *H*,^{5} *H*^{6} −Phen), 7.97 (d, J = 9.4 Hz, 2H, *H*,^{4} *H*^{7} −Phen), 8.31 (d, J = 9.4 Hz, 2H, *H*^{3}, *H*^{8} −Phen). MS−FAB(+) *m*/*z* 779 [(M + Na^+], 754 [M]. Calcd. for $C_{38}H_{56}N_6O_{10}$: 754. $C_{38}H_{56}N_6O_{10}$ Calcd: C, 60.29; H, 7.47; N, 11.10. Found: C, 60.64; H, 7.30; N, 10.95.

2,9-Bis-{13-[4′-(1-phenyl-*p*-methylen)-2,2′:6′,2″-terpyridine]-1,7,-10,16-tetraoxa-4,13-diazacyclooctadecane}-carbonyl-1,10-phenanthroline (1). Solid Na_2CO_3 (280 mg, 2.65 mmol) was added to a solution of **5** (400 mg, 0.53 mmol) and **6** (430 mg, 1.06 mmol) in CH_3CN (50 mL), and the resulting suspension was stirred at reflux for 48 h. The reaction mixture was allowed to cool to room temperature, and the solvent was evaporated in vacuo. The residue was taken up with 100 mL of CH_2Cl_2, filtered through a Celite plug, and the solvent evaporated to afford **1** (0.71 g, yield = 95%) as a light yellow spongy solid. ^{1}H NMR ($CDCl_3$): δ 2.62−2.87 (m, 8H, C*H*$_2$N), 3.15−4.15 (m, 44H, C*H*$_2$O, C*H*$_2$NCO, C*H*$_2$C$_6$H$_4$), 7.26−7.50 (m, 8H, H,^{5} H$^{5''}$ − Terpy, H^3, H^5 − C$_6$H$_4$), 7.75−7.95 (m, 10H, H$^{3''}$, H$^{6''}$ −Terpy, *H*,^{5} *H*^{6} −Phen, H^2, H^6 − C$_6$H$_4$), 8.05 (d, J = 9.4 Hz, 2H, *H*,^{4} *H*^{7} −Phen), 8.40 (d, J = 9.4 Hz, 2H, *H*^{3}, *H*^{8} −Phen), 8.60−8.75 (m, 12H, H^3, H,^{6} H$^{3'}$, H$^{5'}$, H$^{3''}$, H$^{6''}$ − Terpy). MS−FAB(+) *m*/*z* 1420 [(M − 1) + Na^+], 1398 [M − 1]. Calcd. $C_{82}H_{86}N_{12}O_{10}$: 1399. $C_{82}H_{86}N_{12}O_{10}$ + NaBr + H_2O Calcd: C, 64.76; H, 5.84; N, 11.04. Found: C, 64.53; H, 5.31; N, 10.99.

[Zn(1)](PF$_6$)$_2$. A mixture of zinc acetate (3 mg, 0.0143 mmol) and **1** (20 mg, 0.0143 mmol) was refluxed in MeOH (10 mL) for 3 h. After cooling to room temperature, the solution was filtered and solid NH_4PF_6 was added. The complex so obtained was collected and purified by recrystallization from CH_3CN/EtOH (yield = 78%). Anal. Calcd for $C_{82}H_{86}F_{12}N_{12}O_{10}P_2Zn$: C, 56.12; H, 4.94; N, 9.58. Found: C, 55.97; H, 4.86; N, 9.49. TOF−SIMS (time-of-flight secondary ion mass spectrometry): [M − 2PF_6 − H]$^+$, calcd 1464, found 1464; [M − 2PF_6 + F]$^+$, calcd 1484, found 1483. The ^{1}H NMR data in acetonitrile solution are reported in ref 16.

[(bpy)$_2$Ru(μ-1)Ru(bpy)$_2$](PF$_6$)$_4$ (Ru2). A solution of Ru(bpy)$_2$Cl$_2$ (15 mg, 0.0286 mmol) and $AgNO_3$ (10 mg, 0.0572 mmol) in 3 mL of H_2O/EtOH 1:1 was added dropwise to a stirred, refluxing solution of **1** (20 mg, 0.0143 mmol) in 4 mL of H_2O/EtOH 1:1, and the mixture was refluxed for an additional 48 h. After cooling to room temperature, the AgCl precipitate was removed by repeated centrifugation, and an excess of solid NH_4PF_6 was added to the concentrated solution. The resulting orange precipitate was filtered off and further purified by column chromatography on Sephadex G-15, eluting with acetonitrile. Yield: 75%. Anal Calcd. for $C_{122}H_{118}F_{24}N_{20}O_{10}P_4Ru_2$: C, 52.21; H, 4.24; N, 9.98. Found: C, 52.02; H, 4.06; N, 9.88. ^{1}H NMR (CD_3CN): δ 2.95−4.23 (m, 52 H, C*H*$_2$N, C*H*$_2$O, C*H*$_2$NCO, C*H*$_2$C$_6$H$_4$), 6.76−9.25 (m, 66 H, Ph, terpy, phen, bpy). TOF−SIMS: [M − PF_6]$^+$, calcd 2661, found 2661; [M + PF_6]$^-$, calcd 2951, found 2951.

[{(bpy)$_2$Ru(μ-2,3-dpp)}$_2$Ru(μ-1)Ru{(μ-2,3-dpp)Ru(bpy)$_2$}$_2$](PF$_6$)$_{12}$ (Ru6). The same procedure employed for **Ru2** was used, with [Cl$_2$Ru{(μ-2,3-dpp)Ru(bpy)$_2$}$_2$](PF$_6$)$_4$ (58.5 mg, 0.0286 mmol), $AgNO_3$ (9.7 mg, 0.0572 mmol) and **1** (20 mg, 0.0143 mmol) in 15 mL of H_2O/EtOH 1:1. After removal of AgCl and addition of NH_4PF_6, a violet powder was isolated. Yield: 79%. Anal. Calcd for $C_{218}H_{190}F_{72}N_{44}O_{10}P_{12}Ru_6$: C, 44.14; H, 3.23; N, 10.39. Found: C, 44.32; H, 3.42; N, 10.36. ^{1}H NMR (CD_3CN): δ 2.91−4.13 (m, 52 H, C*H*$_2$N, C*H*$_2$O, C*H*$_2$NCO, C*H*$_2$C$_6$H$_4$), 6.74−9.54 (m, 138 H, Ph, terpy, phen, bpy, μ-2,3-dpp). TOF−SIMS: [M − PF_6]$^+$, calcd 5790, found 5790; [M + PF_6]$^-$, calcd 6080, found 6080.

Acknowledgment. We thank the Italian Ministero dell′Università e della Ricerca Scientifica e Tecnologica (MURST, special program on "Dispositivi supramolecolari"), the Consiglio Nazionale delle Ricerche (CNR), and the European Community TMR Program (Research Network on Nanometer Size Metal Complexes) for financial support.

IC010338+